Supplementary Material

Dual defect sites at g-C_3N_4 synergistically induced the electron localization effect for boosting photocatalytic H_2O_2 production

Jingjing Jiang [a], Yuyao Chen [a], Shijian Zhou [a *], Haoran Xie [a], Changlai Li [a], Zheng , Wei [a], Yan Kong [a, *]

[a] *State Key Laboratory of Materials-Oriented Chemical Engineering, College of Chemical ·Engineering, Nanjing Tech University, Nanjing 211816, China*

[*] Corresponding author, Email:

zshijian@njtech.edu.cn (Prof. Shijian Zhou);

kongy36@njtech.edu.cn (Prof. Yan Kong);

Table of contents

1. Reagents and materials

Urea (CH_4N_2O), thioacetamide (C_2H_5NS), isopropanol (IPA), *p*-benzoquinone (p-BQ), silver nitrate ($AgNO_3$), potassium iodide (KI), potassium hydrogen terephthalate ($KC_8H_5O_4$) and deionized water were obtained from Sinopharm Chemical Reagent Co., Ltd. (Shanghai, China). All reagents used in this study were of commercially available analytical grade.

2. Characterizations

2.1 Characterization of materials

The crystalline structures were determined using powder X-ray diffraction (XRD, Smart Lab 9 kW, Japan) patterns, with a Cu Kα radiation (λ=0.154168 nm) at 40 kV and 100 mA. The chemical compositions, states, and valence band of the catalysts were carried out by X-ray photoelectron spectroscopy (XPS, ESCALAB 250Xi, USA) using Al Kα radiation, and all binding energies were referenced to the C1s peak 3 at 284.8 eV. The morphology was investigated by a field-emission scanning electron microscope (FESEM, Hitachi S4800, Japan). UV–Vis absorption spectra were measured by a Lambda 950 ultraviolet–visible diffuse reflectance spectrophotometer (UV–vis DRS) using $BaSO_4$ as reference. Electron spin resonance (ESR) signals of the radicals captured by DMPO were measured in a Bruker A300 spectrometer (Germany). Set the center field to 3502 G, sweep width to 100 G, microwave frequency to 9.83 GHz.

2.2 Electrochemical test

The electrochemical tests involved in this study include: Transient photo-current, Electrochemical impedance spectra (EIS) and Linear sweep voltammetry (LSV) curves are performed using an electrochemical workstation (Chenhua CHI760E). Transient

photo-current and EIS tests are used to analyze the photoelectric signals on the catalyst surface. The Transient photo-current evaluates the photoresponsivity of the catalyst and the carrier migration rate, while the EIS reflects the charge transfer resistance of the material interface. Both of the above electrochemical tests were performed using a standard three-electrode system in 0.2 M sodium sulfate electrolyte with Ag/AgCl electrode as the reference electrode, Pt electrode as the counter electrode, and sample electrode as the working electrode. The working electrode was prepared as follows: 5 mg of the sample was fully dispersed in 1 mL of 10% Nafion solution, followed by taking 10 μL of the slurry and applying it on the FTO (Fluorine-doped tinoxide) glass (the coating area was 1 × 1 cm), and finally, the prepared electrode was placed to dry for 12 h at 80 °C.

The LSV curves are tested using Rotating disk electrode (RDE) to evaluate the ORR process of the catalyst during the photocatalytic H_2O_2 evolution. Again, Ag/AgCl electrode Is used as the reference electrode, Pt electrode as the counter electrode and sample electrode as the working electrode. The working electrode is prepared in a similar way as described above except that the coating is changed to circular glassy carbon with a diameter of 5 mm. The LSV curves are performed in phosphate buffer (pH=7) with saturated oxygen concentration at a scanning rate of 10 mV s^{-1}. The average number of electron transfers (n) involved in oxygen during the ORR process can be fitted by the following equation:

$$j^{-1} = j_k^{-1} + B^{-1}\omega^{-1/2}$$

$$B = 0.2nF\nu^{-1/6}CD^{2/3}$$

where j is the tested current density; j_k is the kinetic current density; ω is the rotational speed (rpm); F is Faraday's constant (96485 C mol^{-1}); ν is the kinetic viscosity of water (0.01 cm^2 s^{-1}); C is the concentration of O_2 in water (1.26×10^{-3} mol cm^{-3}); and D is the diffusion velocity of O_2 (2.7 × 10-5 cm^2 s^{-1}).

3. Photocatalytic performance tests

The photocatalytic H_2O_2 production experiments were carried out as follows: 15 mg of catalyst was dispersed in 30 mL of aqueous solution containing 10 vol% isopropanol (IPA) with ultrasonication for 5 min. Then a 300 W Xe lamp (Beijing, CEL-HXF-300) with a 420 nm cutoff filter was used to obtain the visible light. Prior to irradiation, the reactor was stirred under dark conditions for 30 min to achieve an equilibrium of adsorption and desorption between the catalyst and the reactants. During the photocatalytic experiment, the solution was sampled at certain time intervals of 15 min by using a 5 mL syringe, and the photocatalysts were removed by using a 0.22 μm Millipore filter. Then, the solution was diluted for measuring the concentration of H_2O_2.

3.1 H_2O_2 detection

The concentration of hydrogen peroxide produced by the reaction was calibrated by iodometry. Configuring KI solution and $C_8H_5KO_4$ solution with concentrations of 0.1M and 0.4M respectively. Then, 1mL KI and 1mL $C_8H_5KO_4$ were added to 2 mL reaction solution successively, and the mixture was placed in a dark place for 30 min. Finally, ultraviolet visible spectrophotometer was used to detect the mixed solution, and the generated hydrogen peroxide content was measured at the concentration reduced to I^{3-}. The process involves the following reactions:

$$H_2O_2 + 3I^- + 2H^+ \rightarrow I^{3-} + 2H_2O$$

Standard curve of UV absorption intensity of I and H_2O_2 concentration:

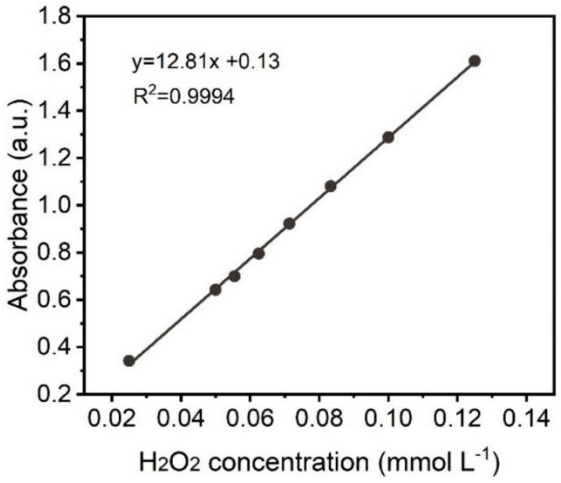

3.2 The Apparent quantum yields (AQY) measurement

A 300 W Xenon lamp (CEL-HXF300) equipped with bandpass filters of different wavelengths is used to direct the photochemical reactor, and the vertical distance between the light source and the reactor quartz lid is fixed during the reaction. The central wavelengths of the bandpass filters are 420, 450, 500, 600, and 700 nm, respectively, and the corresponding optical power densities are 10.2, 14.8, 22.2, 59.9, and 77.4 W m^{-2}, respectively. The AQY value is calculated by the following formula:

$$AQY = \frac{N_{H_2O_2}}{N_P} = \frac{2N_a \times M_{H_2O_2} \times hc}{PSt\lambda}$$

Where, M corresponds to the content of hydrogen peroxide (mmol) produced in the photocatalysis process; Na is Avogadro's constant (6.022×10^{23} mol^{-1}). h is the Planck constant (6.626×10^{-34} J S), c is the speed of light (3×10^8 m s^{-1}), S is the radiation area of the photoreactor (the effective radiation area of the photochemical reactor in this paper is 19.6 cm^2), t is the reaction time (s); λ is the wavelength of monochromatic light(m).

3.3 The solar-to-chemical energy conversion (SCC) efficiency measurement

The 15 mg catalyst was well dispersed in 30 mL deionized water and degassed by O^2 bubbling for 30 min before being sealed in vessel. A 300 W Xe lamp (Beijing, CEL-HXF-300) was used as the light source. The reaction temperature was kept at 25°C. The SCC efficiency was calculated via the following equation:

$$SCC = \frac{\Delta G \times M_{H_2O_2}}{total\ input\ energy \times t}$$

Where, ΔG is the free energy for H_2O_2 formation (117 kJ mol^{-1}).

4.Fig.S1-7

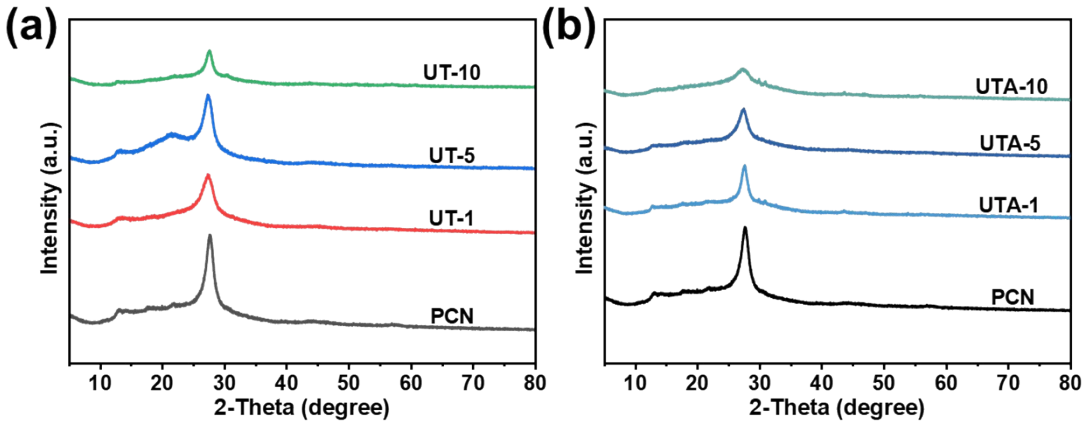

Fig. S1 XRD patterns of different samples.

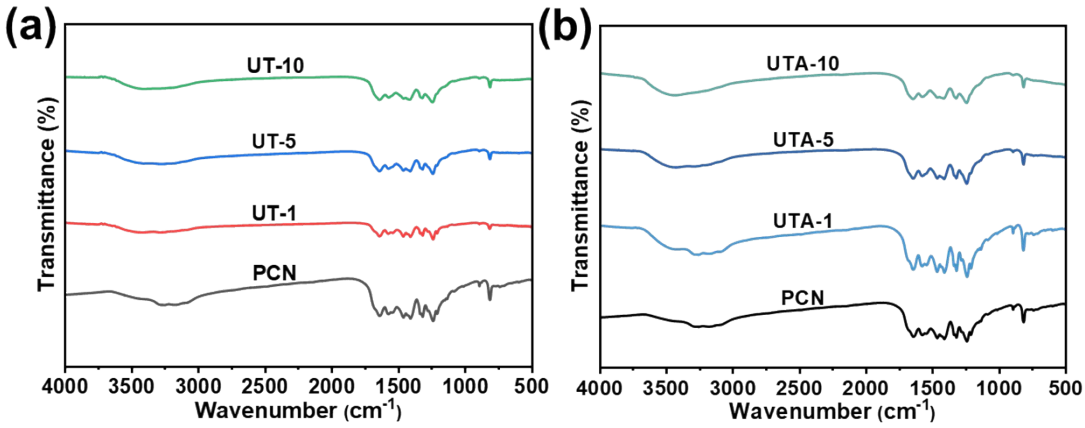

Fig. S2 FT-IR spectra of different samples.

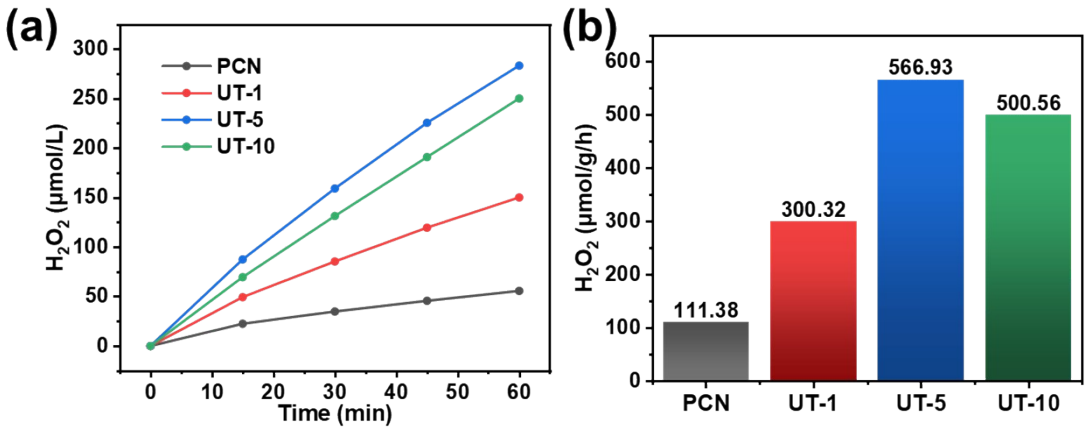

Fig. S3 Photocatalytic performance of H_2O_2 of different samples under (a)the pure water and (b)the 10% IPA aqueous solution.

.

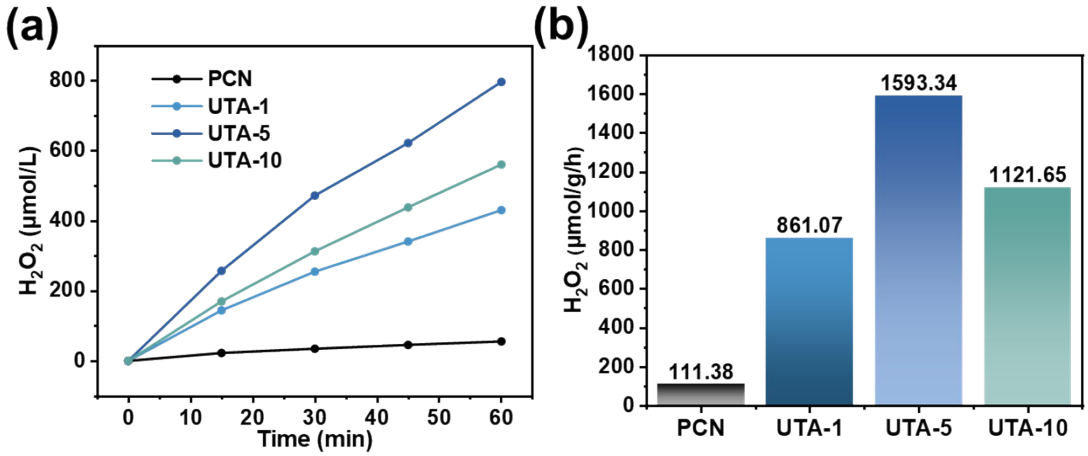

Fig. S4 Photocatalytic performance of H_2O_2 of different samples under (a)the pure water and (b)the 10% IPA aqueous solution.

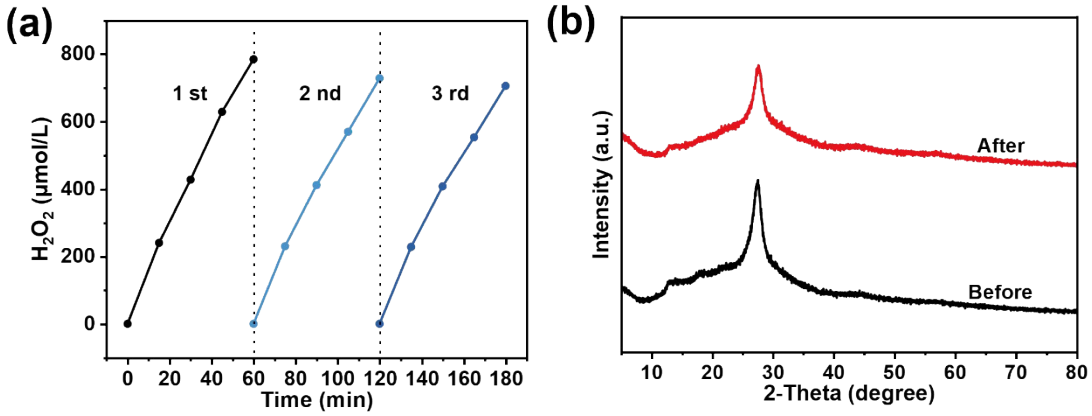

Fig. S5 (a) three cycle experiments of UTA-5, (b) XRD spectra of UTA-5 before and after cycling experiments.

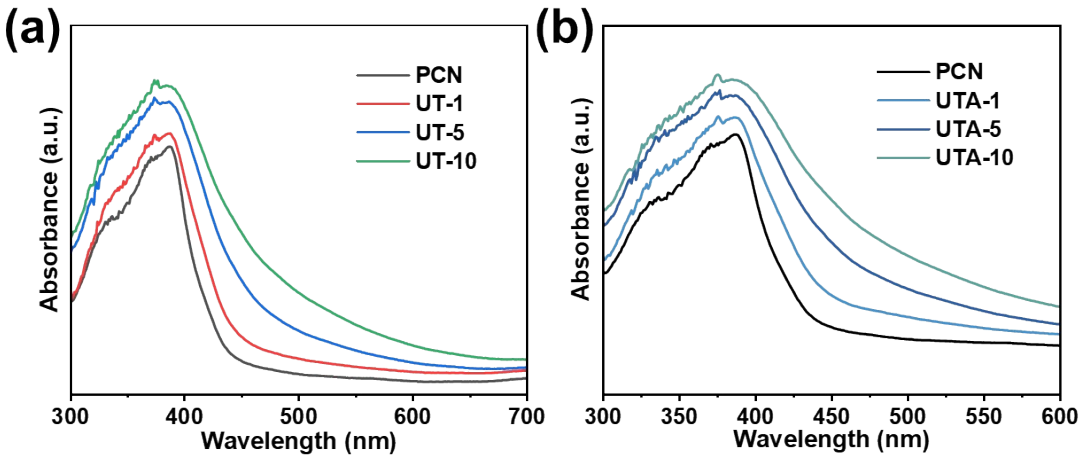

Fig. S6 (a, b) UV-vis DRS of different samples.

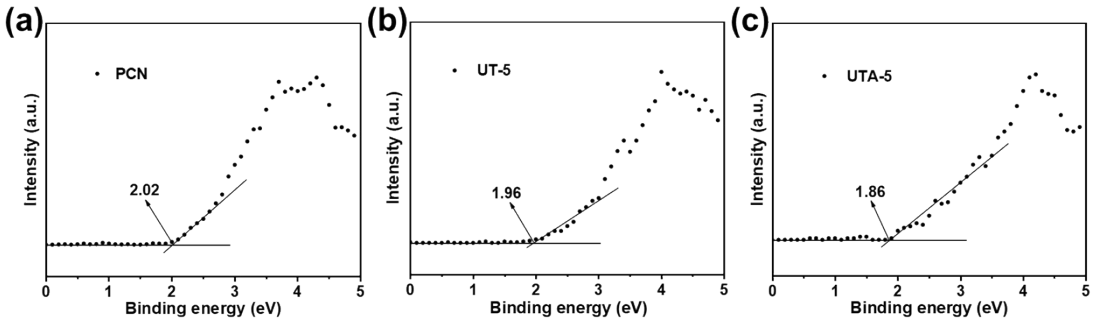

Fig. S7 VB-XPS of (a) PCN, (b) UT-5, (c) UTA-5.

5. Table S1-2

Table S1 XPS atomic ratios and S content based on ICP in different samples

Sample	N/C	N_{2C}/N_{3C}	S (ICP-MS wt%)
PCN	1.45	2.22	~
UT-5	1.35	2.50	0.23
UTA-5	1.05	2.94	0.22

Table S2 Performance of photocatalytic H_2O_2 production in comparison with metal-free g-C_3N_3.

Sample	Reaction solution	Light source	H_2O_2 (μmol g^{-1} h^{-1})	Atmosphere	Ref.
P/g-C_3N_4	10vol% EtOH	visible light (λ≥420nm,100 mW cm^{-2})	730.11	O_2	[1]
oc-g-C_3N_4-0.8	10vol% EtOH	LED light source (100 Mw cm^{-2},420 nm)	533.33	O_2	[2]
CN-HP	10vol% IPA	300 W xenon lamp (providing visible light λ > 420 nm)	244.8	O_2	[3]
O-CNC	10vol% IPA	simulated solar light irradiation	2008.4	O_2	[4]
CNT	10vol% IPA	a light source of AM 1.5 (100 mW cm^{-2}, 400 nm ≤ λ ≤760 nm)	490	O_2	[5]
N-C@CNHS	10vol% IPA	A xenon lamp (100 mW cm^{-2}; with a 420 nm filter)	4568	O_2	[6]
H-CN	10vol% IPA	300mW xenon lamp (λ > 420 nm)	718.36	O_2	[7]

g-C_3N_4-TP	10vol% IPA	LED (λ>420 nm)	552	O_2	[8]
M-CN	10vol% IPA	350 W Xenon lamp (λ>420 nm)	785	O_2	[9]
SPCN	10vol% IPA	300 W white-light light emitting diode (LED)	323.6	O_2	[10]
P-CN	10vol% IPA	visible light (Xe lamp, λ> 420 nm)	649.5	O_2	[11]
B-CNT	10vol% IPA	simulated solar light	915.49	O_2	[12]
UTA-5	10vol% IPA	300W Xe lamp (λ>420 nm)	1593.34	O_2	This work
UT-5	10vol% IPA	300W Xe lamp (λ>420 nm)	566.93	O_2	This work
PCN	10vol% IPA	300W Xe lamp (λ>420 nm)	111.38	O_2	This work

References

1. X. Xu and Z. Zhang, *Catalysis Science & Technology*, 2024, **14**, 3374-3381.
2. Q. Hu, Y. Dong, K. Ma, X. Meng and Y. Ding, *Journal of Catalysis*, 2022, **413**, 321-330.
3. T. Ge, X. Jin, J. Cao, Z. Chen, Y. Xu, H. Xie, F. Su, X. Li, Q. Lan and L. Ye, *Journal of the Taiwan Institute of Chemical Engineers*, 2021, **129**, 104-111.
4. H. Xie, Y. Zheng, X. Guo, Y. Liu, Z. Zhang, J. Zhao, W. Zhang, Y. Wang and Y. Huang, *Acs Sustainable Chemistry & Engineering*, 2021, **9**, 6788-6798.
5. J. Chen, W. Gao, Y. Lu, F. Ye, S. Huang, Y. Peng, X. Yang, Y. Cai, J. Qu and J. Hu, *Acs Applied Nano Materials*, 2023, **6**, 3927-3935.
6. X. Dang, X. Cui, H. Zhang, X. Chen and H. Zhao, *Acs Sustainable Chemistry & Engineering*, 2023, DOI: 10.1021/acssuschemeng.3c03183.
7. Z. Zhang, Y. Zheng, H. Xie, J. Zhao, X. Guo, W. Zhang, Q. Fu, S. Wang, Q. Xu and Y. Huang, *Journal of Alloys and Compounds*, 2022, **904**.
8. Y. Luo, Y. F. Lin, Z. L. Weng, B. Han, Y. Zhou, X. W. Ou and J. Jiang, *Journal of Environmental Chemical Engineering*, 2023, **11**.
9. Y. Zhang, M. Fang, X. Qian, L. Zhang, P. Gu, Y. Liu and H. Yang, *Journal of Materials Research*, 2021, **36**, 3495-3505.
10. W. Miao, Y. Wang, Y. Liu, H. Qin, C. Chu and S. Mao, *Engineering*, 2023, **25**, 214-221.
11. L. Xue, H. Sun, Q. Wu and W. Yao, *Journal of Colloid and Interface Science*, 2022, **615**, 87-94.
12. Y. Liu, Y. Zheng, W. Zhang, Z. Peng, H. Xie, Y. Wang, X. Guo, M. Zhang, R. Li and Y. Huang, *Journal of Materials Science & Technology*, 2021, **95**, 127-135.